NORDITA-FLOW Spring School on Turbulent Boundary Layers
Stockholm, April 6-9th 2010

Compressible Turbulent Boundary Layers (Part 1)

Neil Sandham
University of Southampton

Compressible flow relative to incompressible flow

- Hyperbolic potential flow (compared to elliptic for incompressible flow)
- Finite rate of propagation of pressure
  - Zone of influence, Mach cone
  - Velocity *u*, sound speed *a*

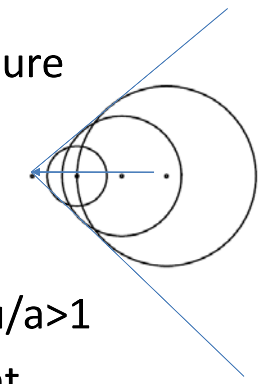

- Possibility of shock waves for M=u/a>1
- Continuity is no longer a constraint

Overview

- Part 1
  - Compressible flow fundamentals
  - Core concepts in compressible boundary layers
  - Canonical flows: boundary layer, channel and mixing layer
- Part 2
  - Applications, focusing on shock-wave/boundary layer interactions
  - Current start of the art

External flow context

Airfoil at incidence; Euler solutions; Mach number contours

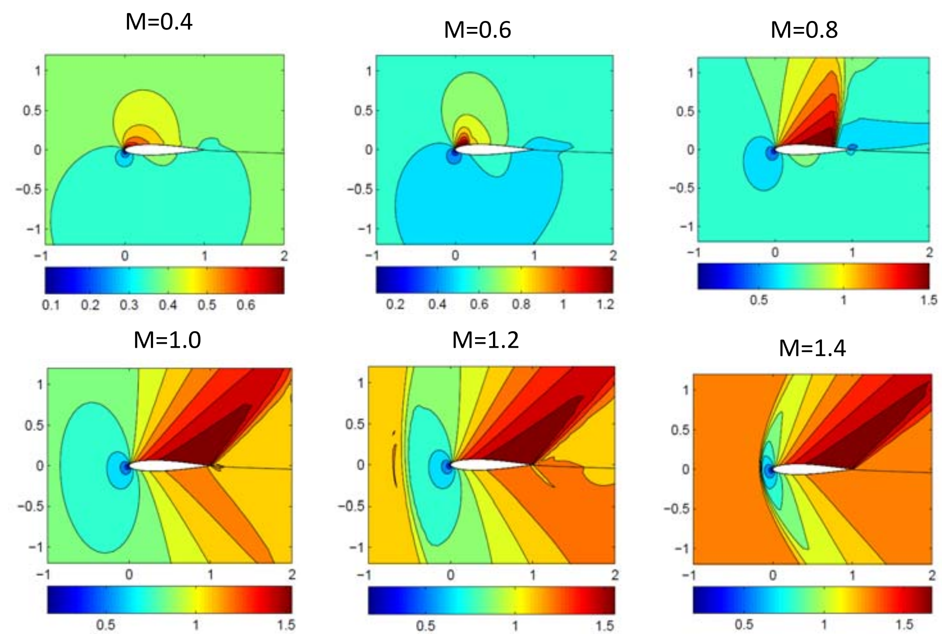

Governing equations

- Mass, momentum and energy conservation

$$\frac{\partial \rho}{\partial t} + \frac{\partial}{\partial x_k}(\rho u_k) = 0,$$

$$\frac{\partial}{\partial t}(\rho u_i) + \frac{\partial}{\partial x_k}[\rho u_i u_k + p\delta_{ik} - \tau_{ik}] = 0,$$

$$\frac{\partial}{\partial t}(\rho E) + \frac{\partial}{\partial x_k}\left[\rho u_k \left(E + \frac{p}{\rho}\right) + q_k - u_i \tau_{ik}\right] = 0,$$

- Note that density is now governed by a transport equation
- Total energy $E = T/[\gamma(\gamma - 1)M^2] + \frac{1}{2}u_i u_i$

Constitutive relations

- Compressible Newtonian fluid

$$\tau_{ik} = \frac{\mu}{Re}\left(\frac{\partial u_i}{\partial x_k} + \frac{\partial u_k}{\partial x_i} - \frac{2}{3}\frac{\partial u_j}{\partial x_j}\delta_{ik}\right)$$

- Fourier heat conduction

$$q_k = \frac{-\mu}{(\gamma - 1)M^2 Pr\, Re}\frac{\partial T}{\partial x_k}$$

Normalised with respect to freestream conditions (velocity, density temperature, viscosity)

Variable viscosity

- Sutherland's law

$$\frac{\mu}{\mu_{ref}} = \left(\frac{T}{T_{ref}}\right)^{3/2}\frac{(T_{ref} + S)}{(T + S)}$$

- Power law

$$\frac{\mu}{\mu_{ref}} = \left(\frac{T}{T_{ref}}\right)^{\Omega}$$

For coefficients see for example the book by F.M.White 'Viscous Fluid Flow'

Final form: Compressible NSE

- Perfect gas $p=\rho RT$
- Constant specific heats (calorically perfect)
- Temperature variation of properties using a constant Prandtl number ($Pr=c_p\mu/\kappa$)
- For extended formulations suitable for hypersonic flow see e.g. Anderson (1989)

Flux vector form of Euler terms

$$U_t + F_x + G_y + H_z = 0$$

$$U = \begin{bmatrix} \rho \\ \rho u \\ \rho v \\ \rho w \\ E_T \end{bmatrix}, \; F = \begin{bmatrix} \rho u \\ \rho u^2 + p \\ \rho u v \\ \rho u w \\ (E_T + p)u \end{bmatrix}, \; G = \begin{bmatrix} \rho v \\ \rho u v \\ \rho v^2 + p \\ \rho v w \\ (E_T + p)v \end{bmatrix}, \; H = \begin{bmatrix} \rho w \\ \rho u w \\ \rho v w \\ \rho w^2 + p \\ (E_T + p)w \end{bmatrix}$$

Form commonly used in CFD (note E_T=E from earlier)

Chu & Kovásznay (1958)

Examples of bilateral interactions of linear modes in compressible flow

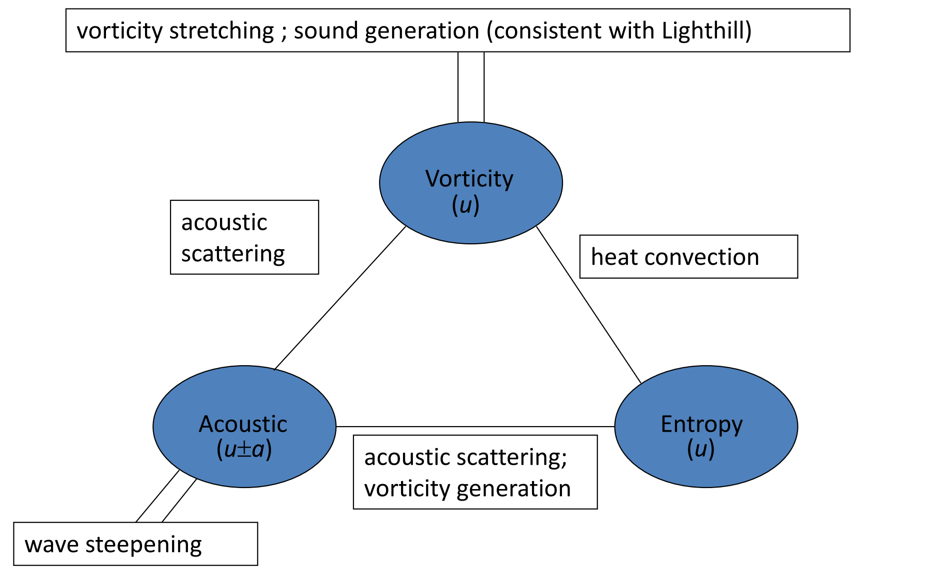

Diagonalisation of Euler terms

- Primitive variable form of Euler equations

$$\frac{\partial U}{\partial t} + A\frac{\partial U}{\partial x} = \ldots \quad \text{with} \quad U = \left(\rho, \;\; u, \;\; v, \;\; p\rho^{-\gamma}\right)^T$$

$$A = T^{-1}\Lambda T \quad \Rightarrow \quad \text{diagonal form}$$

$$\Lambda = (u, \;\; u, \;\; u+a, \;\; u-a)^T$$

- Classify as acoustic, entropy and vortical modes
- Application to characteristic boundary conditions (zero out the rate of change of incoming characteristics)

Reynolds averaging leads to additional compressible terms

- e.g. $\overline{\rho u} = \bar{\rho}\bar{u} + \overline{\rho' u'}$

$$\overline{\rho u v} = \bar{\rho}\bar{u}\bar{v} + \bar{\rho}\overline{u'v'} + \bar{u}\,\overline{\rho' v'} + \bar{v}\,\overline{\rho' u'} + \overline{\rho' u' v'}$$

- Resulting equations of motion become cumbersome

Favre averaging

- Basic decomposition

$$f = \tilde{f} + f'' \quad \text{with} \quad \tilde{f} = \frac{\overline{\rho f}}{\bar{\rho}}$$

- Useful identities

$$\overline{\rho f} = \bar{\rho}\tilde{f}, \quad \overline{f''} = \bar{f} - \tilde{f}, \quad \overline{\rho f''} = 0$$

- Leads to equations with similar form to low-speed, e.g. continuity

$$\frac{\partial \bar{\rho}}{\partial t} + \frac{\partial \bar{\rho}\tilde{u}_k}{\partial x_k} = 0$$

Energy

$$\frac{\partial \bar{\rho}\tilde{E}}{\partial t} + \frac{\partial \bar{\rho}\tilde{u}_j\tilde{H}}{\partial x_j} = \frac{\partial}{\partial x_j}\left(\overline{\sigma_{ij}u_i} - \bar{q}_j - \overline{\rho u_j'' E''}\right)$$

$$\bar{q}_j = -\overline{\kappa \frac{\partial T}{\partial x_j}} \approx -\bar{\kappa}\frac{\partial \tilde{T}}{\partial x_j}$$

$$\text{where} \quad \tilde{H} = \tilde{E} + \frac{\bar{p}}{\bar{\rho}}, \quad \tilde{E} = \tilde{e} + \frac{1}{2}\left(\tilde{u}_i\tilde{u}_i + \frac{\overline{\rho u_i'' u_i''}}{\bar{\rho}}\right)$$

Momentum

$$\frac{\partial \bar{\rho}\tilde{u}_i}{\partial t} + \frac{\partial \bar{\rho}\tilde{u}_i\tilde{u}_j}{\partial x_j} + \frac{\partial \bar{p}}{\partial x_i} = \frac{\partial}{\partial x_j}\left(\sigma_{ij} - \overline{\rho u_i'' u_j''}\right)$$

$$\sigma_{ij} = \overline{2\mu\left(S_{ij} - \frac{1}{3}S_{kk}\delta_{ij}\right)} \approx 2\bar{\mu}\left(\tilde{S}_{ij} - \frac{1}{3}\tilde{S}_{kk}\delta_{ij}\right)$$

$$\text{where} \quad S_{ij} = \frac{1}{2}\left(\frac{\partial u_i}{\partial x_j} - \frac{\partial u_j}{\partial x_i}\right)$$

Compressible turbulent boundary layer flow

- High heating near wall leading to strong temperature and density gradients
- Compressibility effect may be expected to become significant at rms Mach number M'=0.3
  - Measured M' are around 0.2 at M_e=2.9 (Spina et al, 1994)
  - Don't expect large compressibility effects until $M_e$is in the range of 4-5

Morkovin hypothesis

- The direct effects of density fluctuations on turbulence are small if the rms density is small compared to the mean density (Bradshaw, 1977)
  - Boundary layers M<5
  - Single stream jets M<1.5
- Acoustic and entropy modes negligible
- Can simplify equations accordingly

Compressible law of the wall

- Van Driest (1951)

$$\overline{u}_{VD}^{+} = \int_0^{\overline{u}^+} \left(\frac{\overline{\rho}}{\overline{\rho}_w}\right)^{1/2} \mathrm{d}\overline{u}^{+}$$

  - Reasonable collapse of measurements and DNS back to incompressible law of the wall
- Crocco-Buseman mean temperature (see e.g. White; Pr=1 assumed) from integration of

$$\frac{\mathrm{d}^2 T}{\mathrm{d}u^2} = -c_p$$

Reasonable agreement with experiments and DNS as we shall see later

Strong Reynolds Analogy (SRA)

- Application of Morkovin's hypothesis to temperature fluctuations

$$\frac{\sqrt{\overline{T''^2}}}{\tilde{T}} = (\gamma - 1) M^2 \frac{\sqrt{\overline{u''^2}}}{\tilde{u}}$$

$$\frac{\overline{T''u''}}{\sqrt{\overline{T''^2}}\sqrt{\overline{u''^2}}} = -1$$

(useful for inflow fluctuations in simulations)

- For more details see Bradshaw, 1977; Barre et al, 2002

Mixing layer

- Collected experimental results for growth rate (Lele, 1994)
- Convective Mach number (Papamoschou and Roshko, 1988)

$$M_c = \frac{U_1 - U_2}{a_1 + a_2}$$

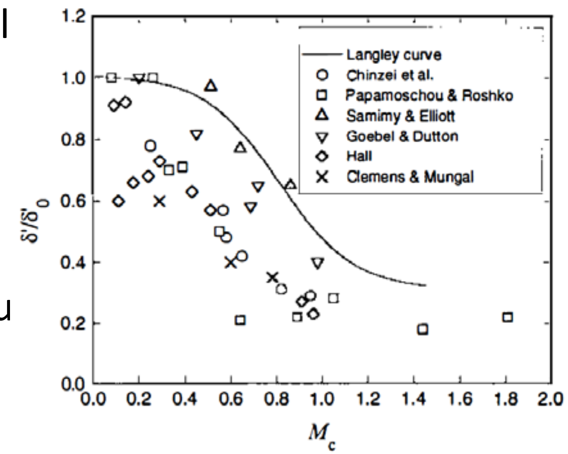

Strong compressibility effect compared to boundary layer (not a mean density effect)

Why is the mixing layer different?

- Large eddies span the whole mixing layer and are exposed to the relative Mach number of the two streams
- Brown-Roshko roller structures are particularly affected

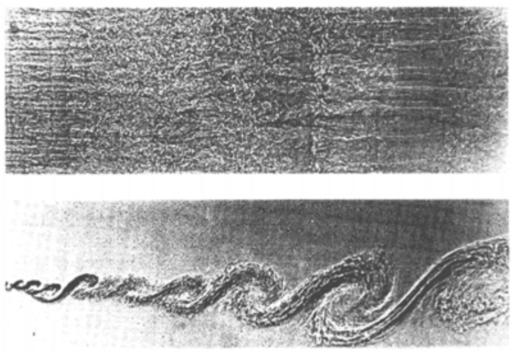

Konrad, experiments 1976 (top and side views)

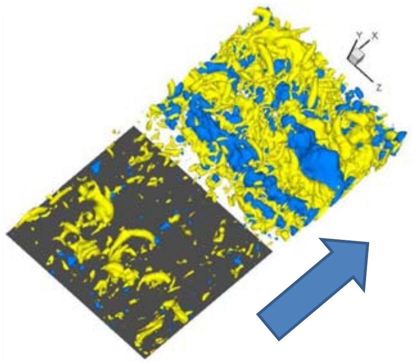

Sandham & Sandberg DNS with splitter plate 2009

Early 1990s modelling attempts

- Dilatation dissipation
  - Include additional dissipation attributed to eddy shocklets (Zeman; Wilcox; Sarkar)

$$\varepsilon_d = f(M_t)\varepsilon$$

- Pressure dilatation
  - Another explicit compressibility term (Sarkar)

Eddy shocklets in mixing layers

2D (M_c=0.8)

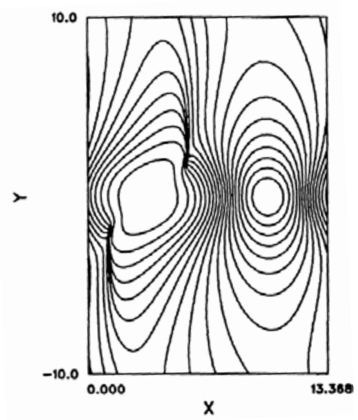

Single structure, time-developing mixing layer (Sandham & Reynolds 1989)

3D (M_c=1.2)

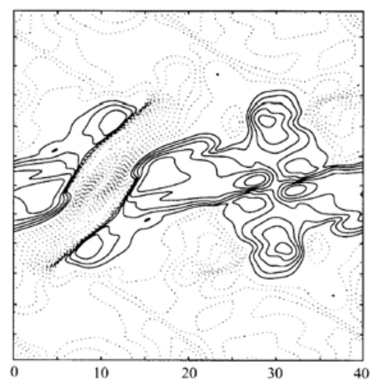

Turbulent flow (Vreman et al 1995)

BUT: These modelling strategies are not supported by DNS of mixing layer

- Vreman et al (1996)
  - Dilatation dissipation insignificant for M_c up to 1.2
  - Pressure dilatation small
- Analysis of integrated equations of motion showed that, for certain assumptions, mixing layer growth rate was instead proportional to the rapid pressure strain term

$$\delta' = -\frac{3}{2\rho_\infty(\Delta U)^2}\Pi_{11}^R$$

Physical mechanism related to pressure fluctuations

- p' reduces with M_c
  - Maximum p corresponds to stagnation conditions
  - Minimum p from a compressible Oseen-vortex model, limited to sonic eddies
  - Absolute limit on p_{min} is $p_\infty (\sim M^{-2})$

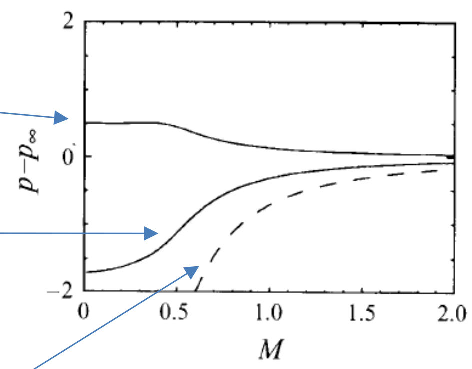

p normalised with $\rho_\infty U_\infty^2$

Connection between linear stability and mixing layer growth rate

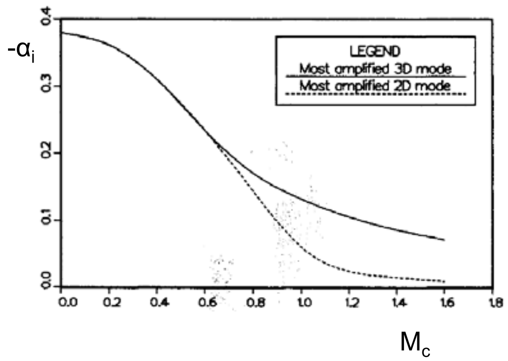

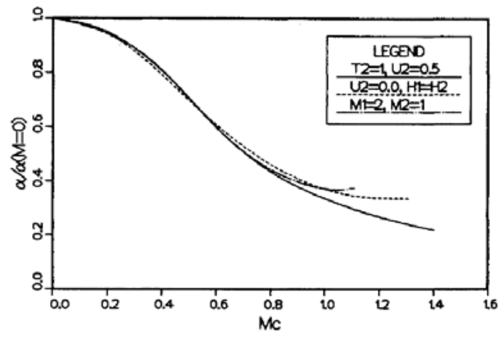

- Note similarity to experimental data
- Derivation by Morris et al (1990): $\frac{d\delta}{dx} \propto (-\alpha_i)$
  - Useful turbulent flow physics from linear theory!

Structural changes in mixing layers

- Increasing three-dimensionality
  - Loss of Brown-Roshko spanwise-coherent roller structures (Sandham & Reynolds 1991; Clemens & Mungal 1995)
  - Emergence of smaller scales with more streamwise orientation
  - Oblique vortices can retain subsonic eddy Mach numbers and avoid strong eddy shock waves

Linear model:

$$\delta'_\rho = -0.6\alpha_{i,\max}$$
$$\delta'_\omega = -0.45\alpha_{i,\max}$$

- Effect of temperature (density) and velocity ratio $\lambda = \frac{U_1 - U_2}{U_1 + U_2}$
  - Compared to Brown & Roshko
- Effect of Mach number
  - Compared to Papamoschou & Roshko

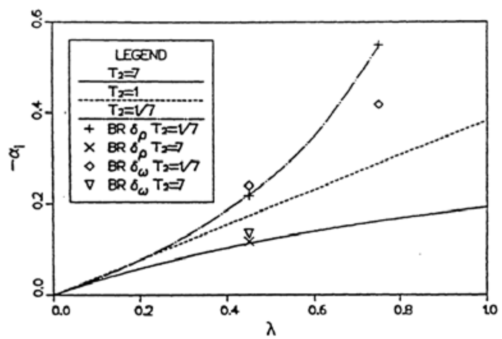

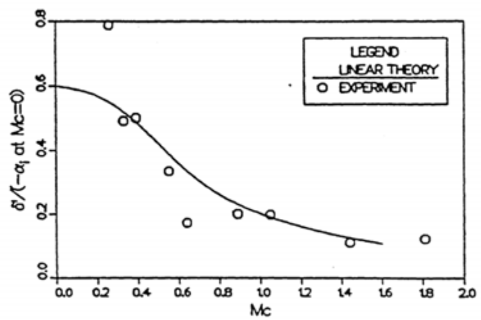

Sandham & Reynolds 1990

Turbulent channel flow

- Coleman, Kim & Moser
  - Simulations with M=1.5 and M=3 compared to incompressible channel flow
  - Isothermal (cold) walls

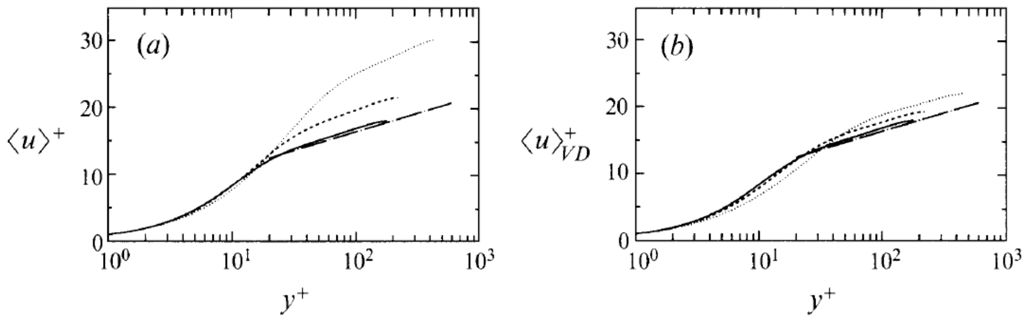

Solid line: M=0, Dashed line M=1.5, Dotted line M=3.0 compared to log law

Structural changes

- Trend towards more coherent low-speed streaks
  - (Coleman et al. channel flow)

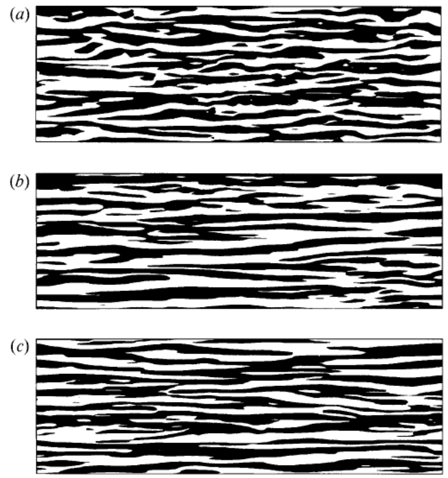

Wall-normal vorticity contours

M=0

M=1.5

M=3.0

Structural changes attributed to mean property variations rather than an intrinsic compressibility effect (still only moderate Mach numbers in the context of Morkovin's hypothesis)

Turbulent channel flow

- Mixed (semi-local) scaling scales the fluctuations (Huang et al, Coleman et al)

Standard

Mixed

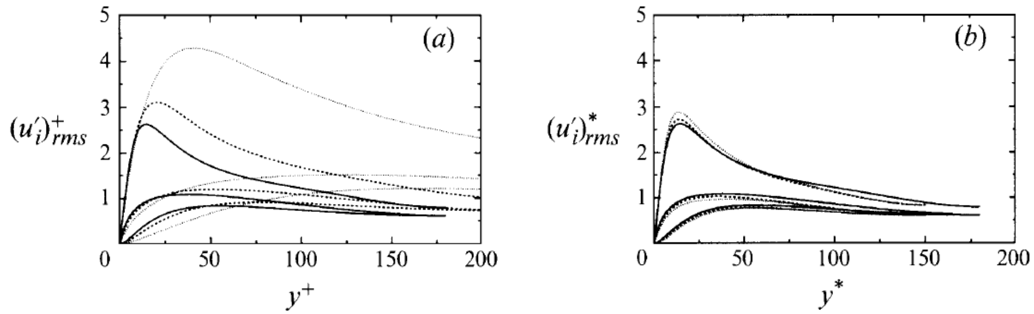

$$u_\tau^*(y) = \left(\frac{\tau_w}{\rho(y)}\right)^2 \qquad u^* = \frac{u}{u_\tau^*} \qquad y^* = \frac{y u_\tau \rho(y)}{\mu(y)}$$

Boundary layer DNS: Mach number effects

- Maeder & Kleiser M_e=3, 4.5 and 6
  - laminar adiabatic wall conditions

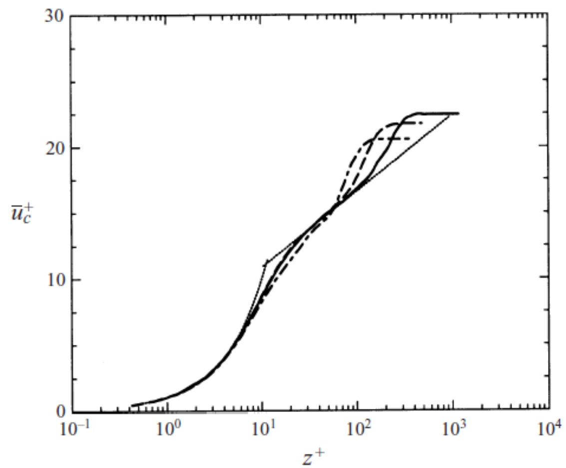

Dilatation dissipation and pressure dilatation terms found to be small

Checks on SRA (Maeder et al)

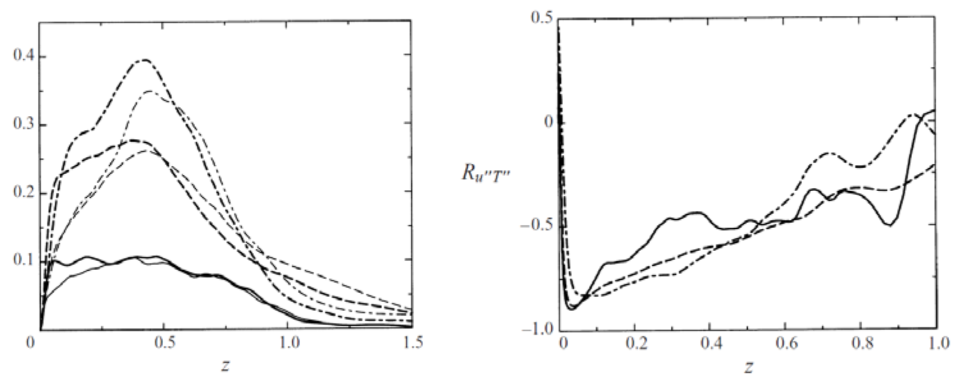

Thick lines r.m.s. $(T'')/\tilde{T}$, thin lines r.m.s. $(T_0'')/\tilde{T}$, ——, case A; – – –, case B; — – —, case C.

Total temperature fluctuations not negligible.
Favre fluctuations in u and T not anti-correlated, except very close to the wall (see also Pirozzoli et al).

Recent experiments show possible wave drag from rough surface (Ekoto et al, 2008)

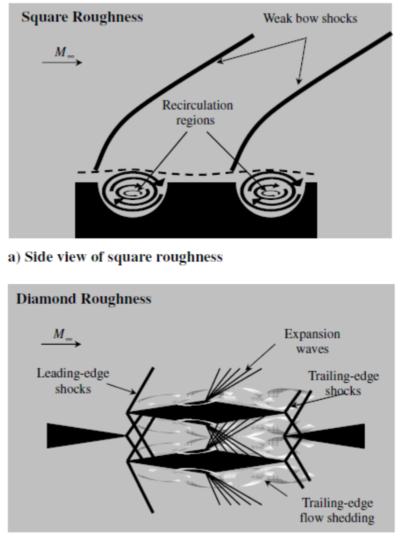

a) Side view of square roughness

b) Top view of diamond roughness

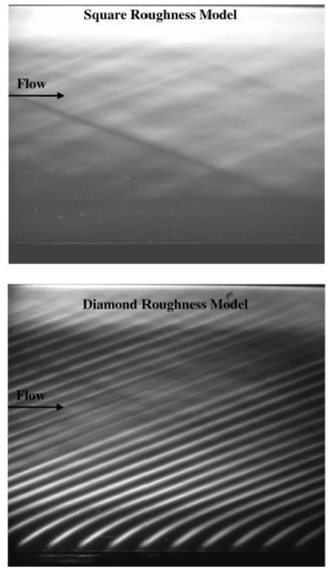

Roughness effects in compressible flow

- Goddard (1959) – wall density scaling

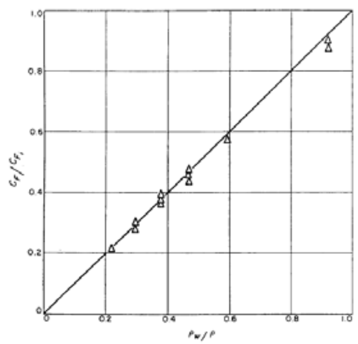

$$\frac{c_f}{c_{f0}} = \frac{\rho_w}{\rho}$$

- But Berg (1979) found predictions a factor of three out for square rods at Mach 6 suggesting additional compressibility effects

References

- Anderson , J. *Hypersonic and High-Temperature Gas Dynamics*, McGraw-Hill.
- Anderson, J. *Modern Compressible Flow*, McGraw-Hill.
- Barre et al, Chapter 10 in *Closure Strategies for Turbulent and Transitional Flows*, CUP Eds Launder & Sandham
- Berg, *AIAA J* 17, 1979
- Bradshaw, P. *Ann. Rev Fluid Mech*. 9, 1977
- Brown & Roshko, *JFM* 64, 1974
- Chu & Kovasznay *JFM* 3, 1958
- Coleman, Kim & Moser *JFM* 305, 1995
- Ekoto, Bowersox, Beutner, Goss, *AIAA J* 46(2), 2008
- Goddard, F. J. Aerospace Sci 26, 1959.
- Huang, Coleman & Bradshaw *JFM* 305
- Lele, *Ann Rev Fluid Mech*. 26, 1994
- Morris, Giridharan & Lilley. *Proc R. Soc. Lond A*, 431, 1990
- Papamoschou & Roshko, *JFM* 197, 1988
- Pirozzoli, Grasso and Gatski, *Phys Fluids* 16, 2004
- Sandham & Reynolds *AIAA J* 28, 1990
- Sandham & Reynolds *JFM* 1991
- Sarkar, S et al, *JFM* 227, 1991
- Sarkar S. *Phys Fluids A* Vol.4, 1992
- Spina, Smits, Robinson *Ann Rev Fluid Mech 26,* 1994
- Van Driest, *J Aero Sci* Vol. 18, 1951 and Vol 23, 1956
- Vreman, Sandham & Luo *JFM* 320, 1996
- White, F. *Viscous Fluid Flow*, McGraw-Hill.
- Wilcox, *AIAA J.* 30, 1992
- Zeman, O *Phys Fluids A.* 2, 1990

NORDITA-FLOW Spring School on Turbulent Boundary Layers
Stockholm, April 6-9th 2010

Compressible Turbulent Boundary Layers (Part 2)

Neil Sandham
University of Southampton

Outline of talk

- Application challenge: scramjet intake
- Bypass transition: turbulent spot and shock/spot interaction
- Shock-turbulence interaction
- Shock/boundary-layer interaction
  - impinging shock
  - ramp

Brief overview of our D/LES approach

- Fourth order accurate space differencing
- Explicit in time RK3 or RK4
- Equation conditioning (entropy splitting, Laplacian formulation of viscous term)
- No filtering or artificial dissipation for DNS
  - local oscillations in DNS if flow under-resolved
- Mixed time scale sub-grid model
  - plus explicit filtering for LES at higher Re
- Shock capturing applied as full-step filter TVD+ACM+Ducros (not applied if no shocks present)

LES sub-grid scale model

Mixed-Time-Scale (MTS) LES model (Inagaki *et al.*, 2005):

$$\nu_t = C_{mts} k_{es} T_s \qquad k_{es} = (\tilde{u}_i - \hat{\tilde{u}}_i)^2$$

$$T_s^{-1} = \left(\frac{\Delta}{\sqrt{k_{es}}}\right)^{-1} + \left(\frac{C_t}{|S|}\right)^{-1},$$

✓Switches off in the laminar regions

✓Localised model

✓No additional damping functions needed near walls

Hypersonic Intake LC01Kx
LAPCAT project

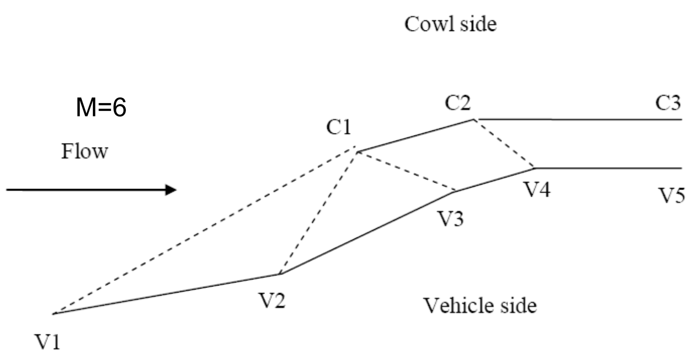

Modified intake without bleed *(A.Mack)*

Two corners V3,V4 spread the pressure rise

- Laminar-turbulent transition along the first ramp (V1-V2).
- Shock-wave interaction with a transitional boundary layer (V2,C2)
- Shock-wave/turbulent boundary-layer interaction near a convex corner (V3,V4).

Krishnan et al 2006

Transition on front ramp

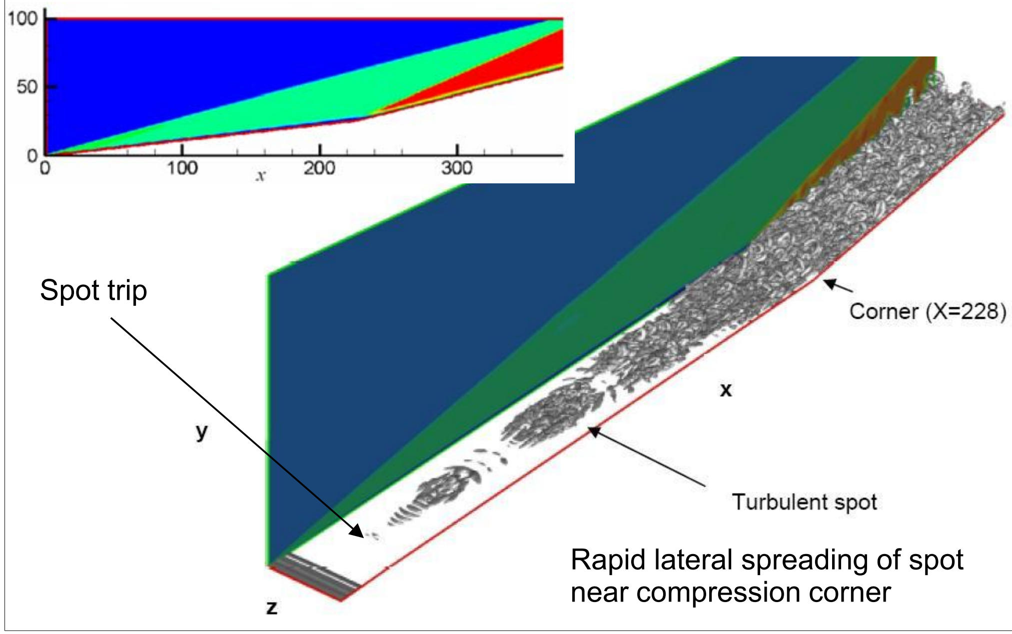

Rapid lateral spreading of spot near compression corner

Simulation details

L_x (mm)	L_y (mm)	L_z (mm)	N_x	N_y	N_z
551.4	106.0	30	999	161	60

Mach	Re_{lref}	T_w/T_∞
6	8399	5.74

Re=4.6 million based on intake length

Local trip (20% Amplitude), 30<x<34 13<z<17 activated for 6 μs at time intervals of 70 μs
31 turbulent spots triggered.

Skin friction distribution

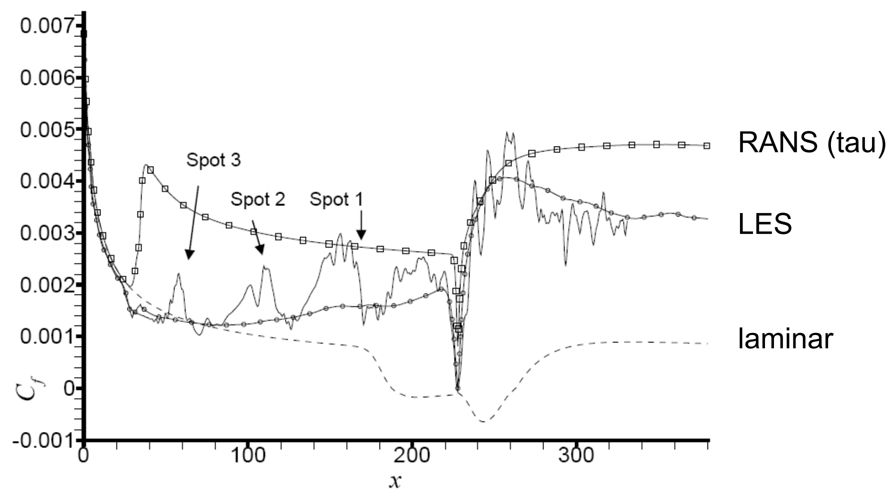

Flow structure inside the intake

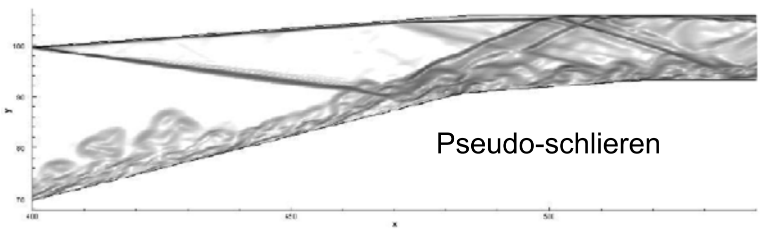

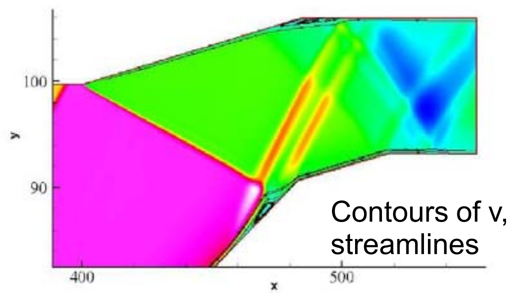

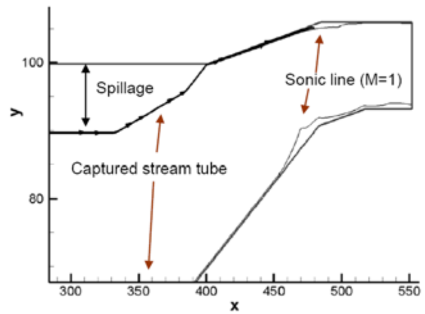

Simplified model problems

- Flat plate turbulent spots
- Spot/shock interactions
- Shock impingement with laminar-turbulent transition
- Shock/isotropic turbulence interaction
- Shock/turbulent boundary layer interactions
  - Compression ramp
  - Shock impingement
  - Flow over a bump

Cowl-side transition

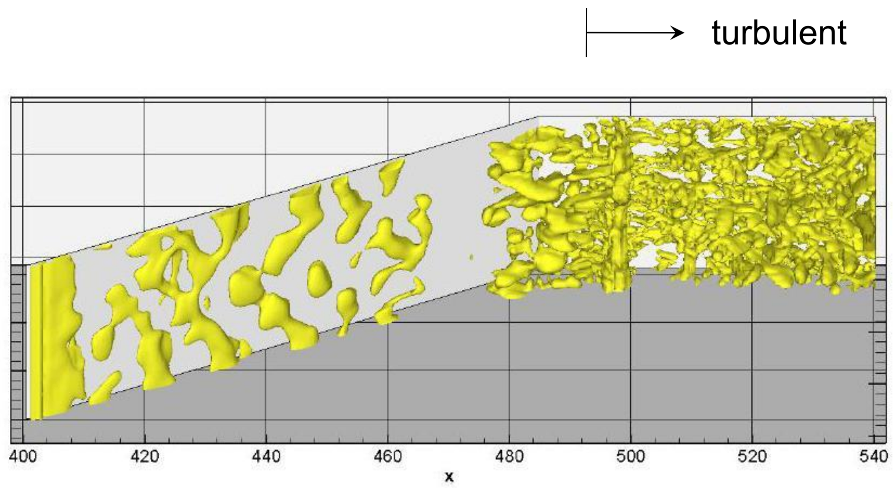

Surface of second invariant

Compressible Turbulent spot DNS

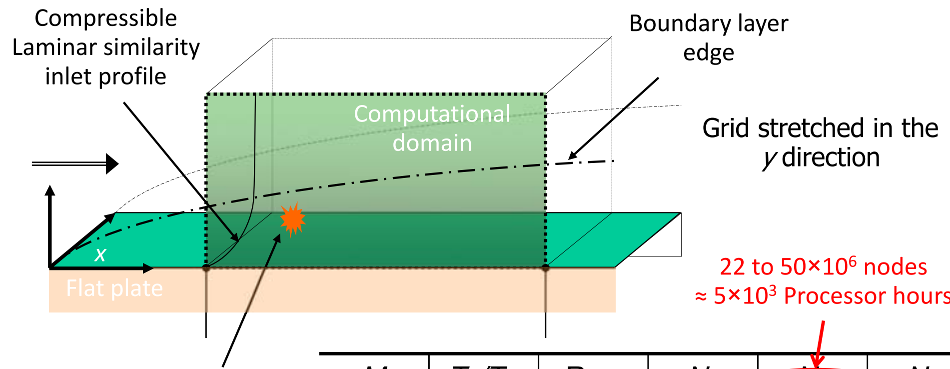

22 to 50×10^6 nodes
$\approx 5\times10^3$ Processor hours

Spot initialization with two vortex pairs (Breuer and Landahl, 1990)

Redford et al (2007)

M	T_w/T_∞	Re_{δ^*}	N_x	N_y	N_z
3	2.5	1500	1101	111	191
	1	1000	1321	111	321
6	7.0	5500	801	141	201
	1	3000	801	141	201

Spot growth

- Most turbulence is created at the wing tip
  – Destabilisation at wing tip (Krishnan & Sandham 2006)
- Turbulence at the front of the spot is convected

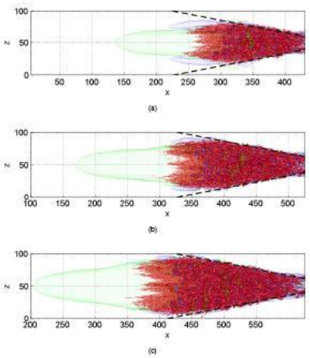

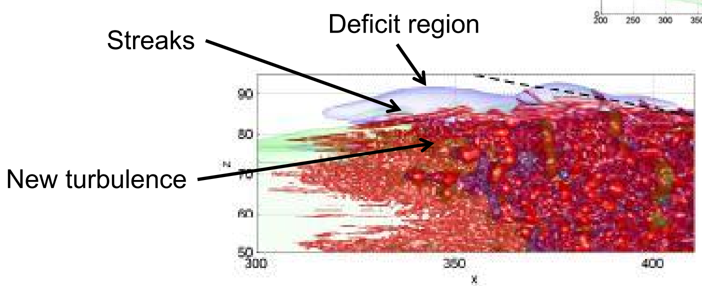

Transitional separation bubble arising from shock impingement

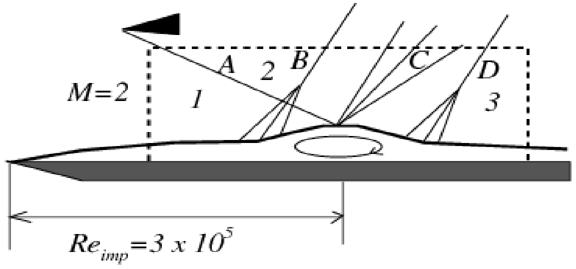

Parameters:
M, p_3/p_1, Re, T_w/T_1

Laminar upstream boundary layer with small disturbances

Differences to low-speed flow:

– density and compressibility affect stability characteristics

– reduced upstream propagation of sound
  - none in freestream
  - sound refraction inside boundary layer

Spot spreading angle

- Spreading angle
  – Reduces with Mach number
  – Cold wall reduces the spread angle by 20-30%
- Measurement variation
  – Jocksch & Kleiser studied Reynolds number effects
  – Differences in measurement techniques

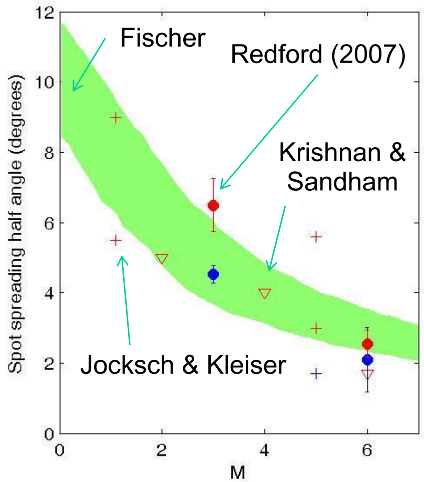

1. Bypass transition: spot/shock interaction

Krishnan & S (2006)

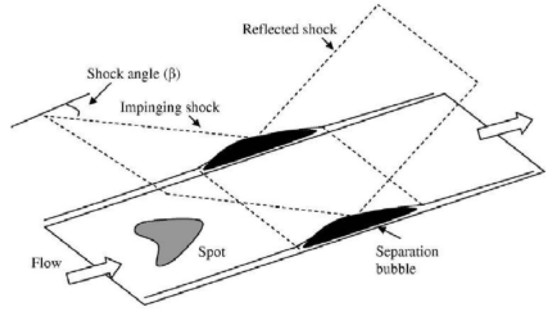

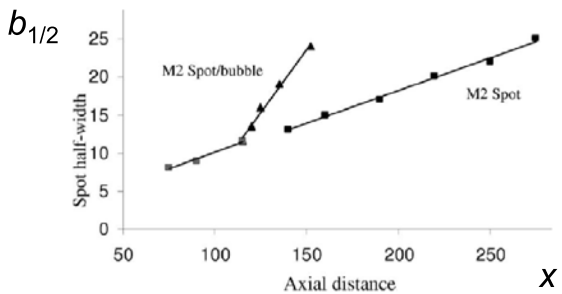

c_f<0

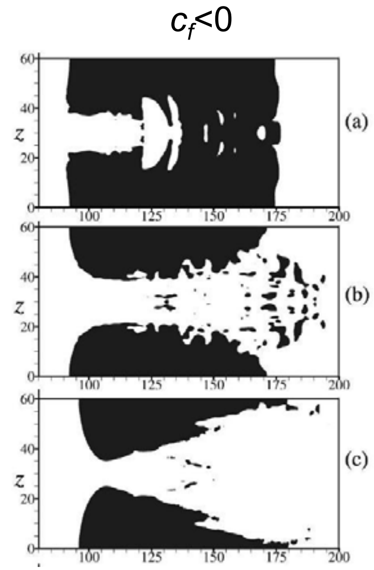

2. Transition via convective instability

Yao et al (PhysFluids, 2007) laminar shock-induced separation bubbles Re_{lb} 2 x 10^5, M=2, p_3/p_1=1.48, T_w=T_{aw} (DNS, LST, PSE, also M=4.5,6.85)

Density:

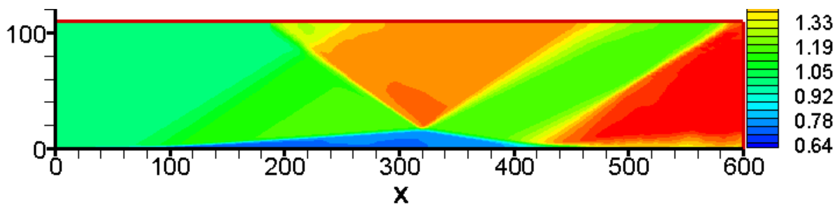

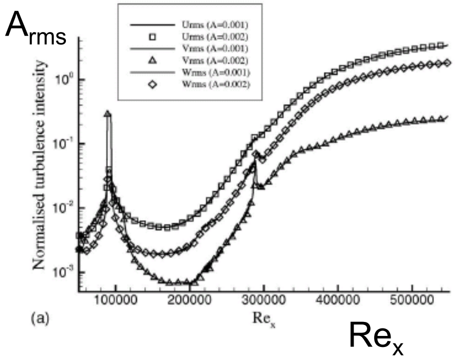

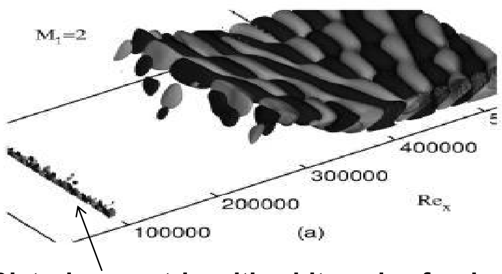

Disturbance strip with white noise forcing

3. Transition via absolute instability

stronger interaction case (Krishnan & S, TSFP 2007)

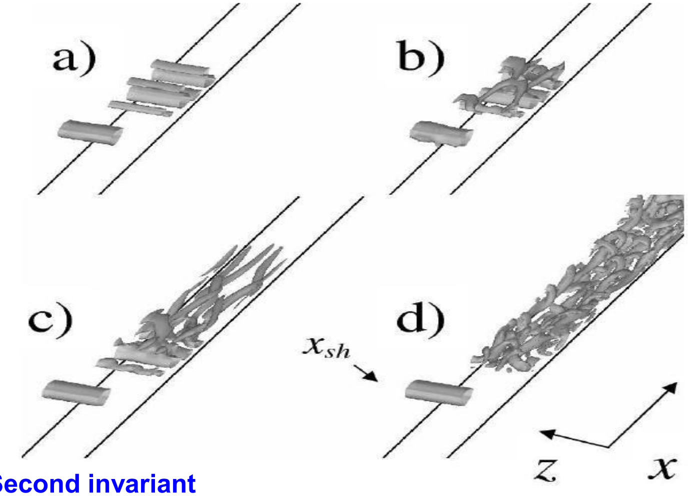

Second invariant

Transition now independent of upstream disturbance amplitude (in agreement with LES of Teramoto, 2005)

Case with higher pressure ratio: P_3/P_1 = 1.91

Long bubble with complex multiple-vortex structure.

L_b/h_b=23.30, L_b/θ_{sep} = 1470; no spontaneous vortex shedding.

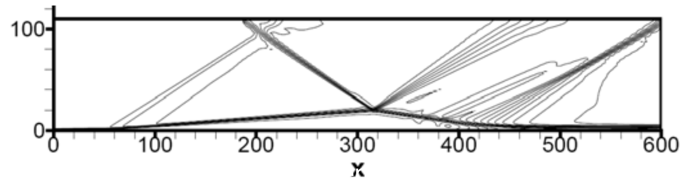

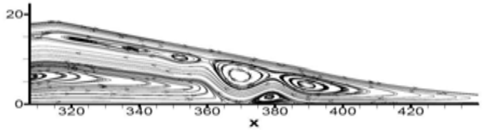

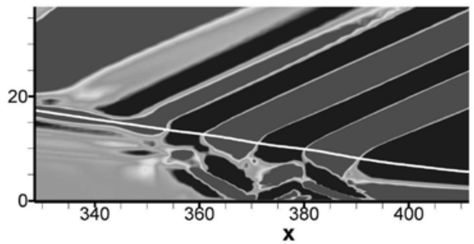

Streamlines (not to scale)

Dilatation rate contours (not to scale)

White line: M = 1

Shock/isotropic turbulence interaction (Lee et al)

- Isotropic decaying turbulence superimposed on stream at M=1.5, 2.0, 3.0
- Decrease in turbulence length scales after shock due to compression
- Amplification of turbulence energy
- Non-polytropic thermodynamic variations downstream of strong shocks

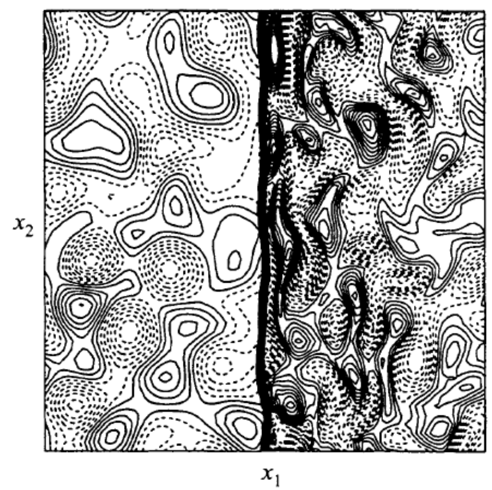

Vorticity contours ω_3

Shock/boundary-layer interactions

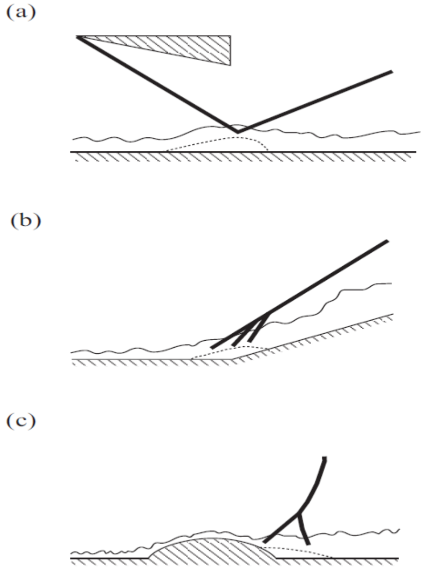

Shock impingement
Laminar or turbulent upstream conditions

Ramp flow

Transonic flow over a bump

Ramp flow (Adams, 2000)

- M=3, 18 degree ramp
  - Turbulent upstream
- Modelling conclusions:
  - Negligible dilatation dissipation
  - Pressure dilatation only significant in separated flow near shock flow
  - SRA questionable

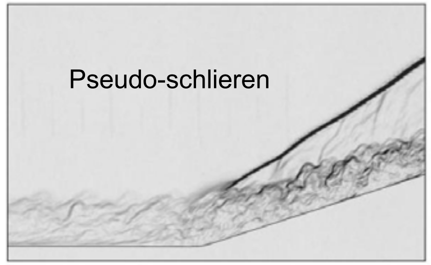

Experiment (25 degree ramp, M=2.9)

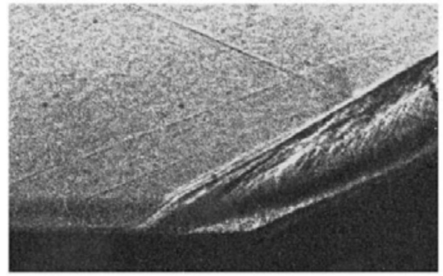

Transonic flow over a bump

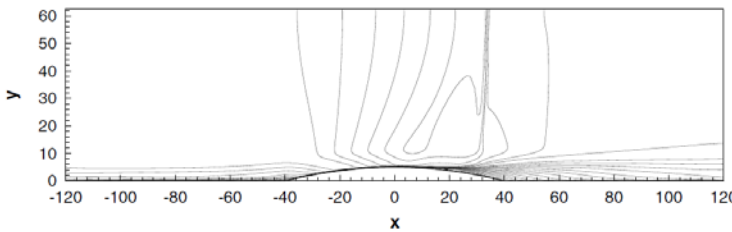

M contours

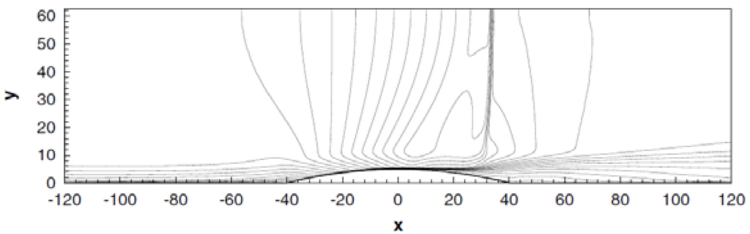

T contours

Shock-induced separation, but LES susceptible to relaminarisation on forward facing slope of bump (Sandham et al 2003)

Ramp flow (Wu & Martin)

- DNS show good agreement with experiment
- Evidence for low-frequency motions, despite short run times of simulations

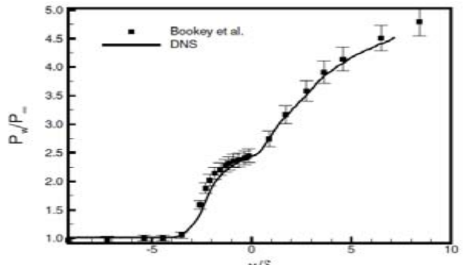

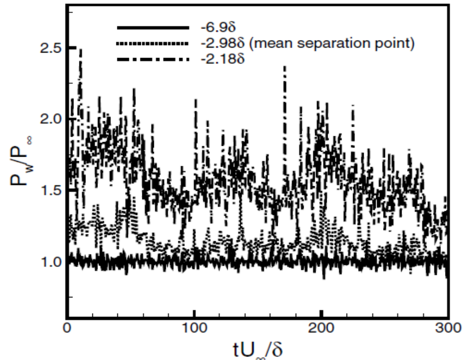

Shock impingement onto turbulent boundary layer Touber & Sandham 2009

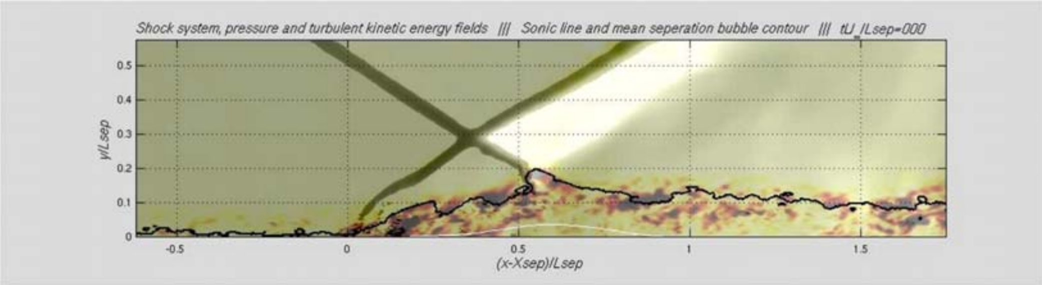

- IUSTI experiment (Dupont et al.)
  - M=2.3, 8 degree shock generator $Re_{\delta 1}$=21000 at x_{imp}, p_3/p_1=2.5
  - Low-f observed near reflected shock foot
- Previous LES by Garnier et al. 2002

  - Box size 71.9x11.2x3.8
  - Grid points 451x81x73
  - Resolution (wall units) 40x1.6x13.5

Grid resolution (2x) and L_z sensitivity

(0.5, 1.0, 5.0$L_{z,ref}$)

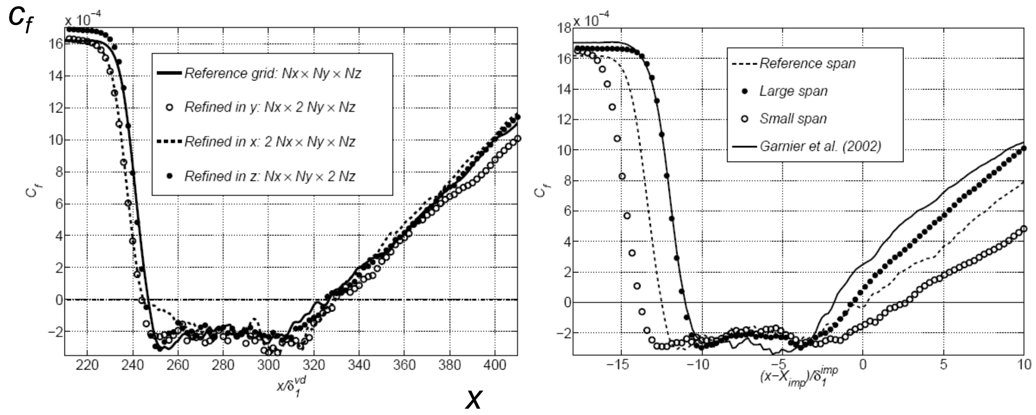

We get a longer bubble with the narrow box, but this configuration allows long run times to study the low-frequency content of the flow

(c_f normalized with properties upstream of interaction)

Inflow turbulence: mean and fluctuations

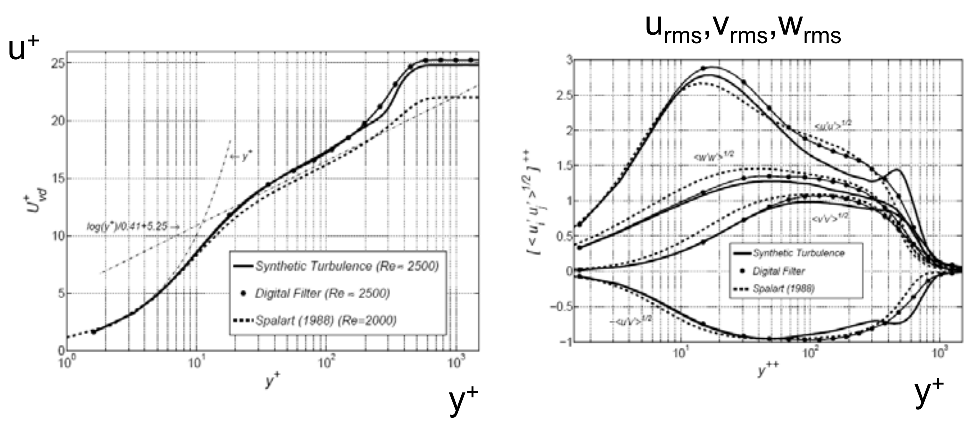

Digital filter and synthetic turbulence alternatives

LES (wide domain) vs PIV (Dupont et al)

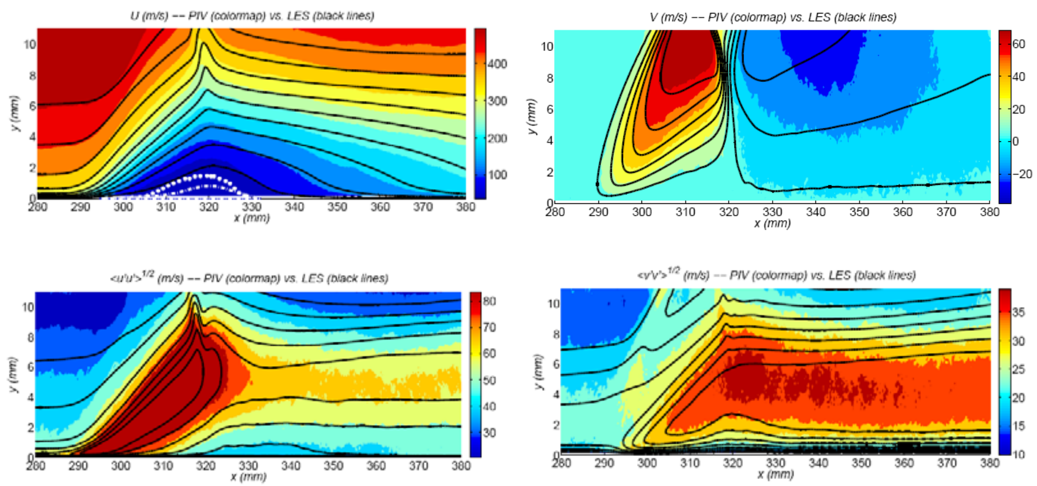

LES (x,y,z): N=451x81x361 L=71.9x11.2x19 (δ_{1i}) Δ^+=40,1.6,13.5

Time traces of wall pressure

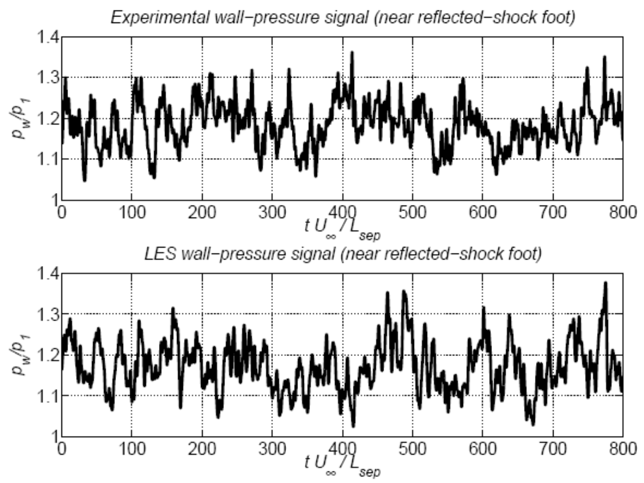

Spatial variation of the power spectrum

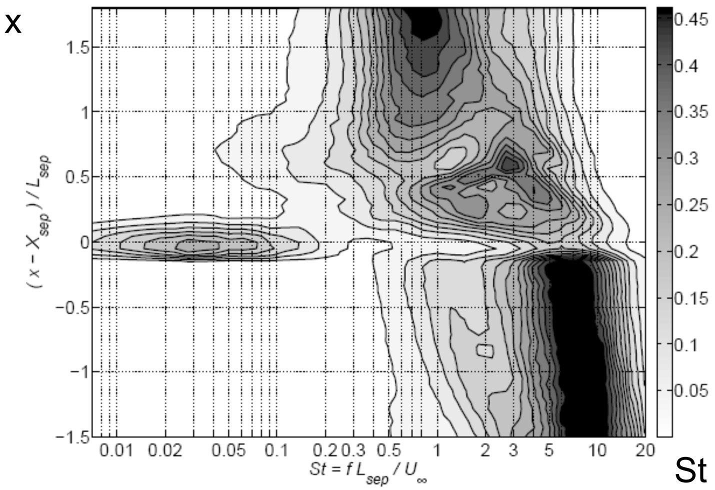

low-f is spatially confined to the foot of the reflected shock

Power spectrum of wall pressure under reflected shock foot

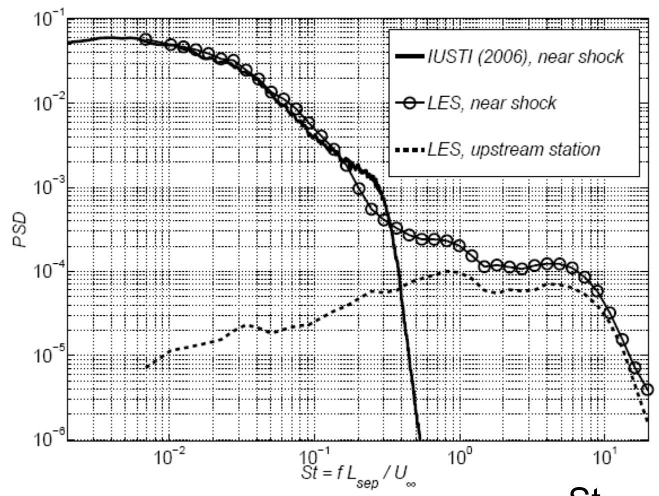

Conclusions

- **Hypersonic intake**
  - Multiple examples of compressibility influences
  - Delayed transition
  - Shock-wave/boundary-layer interaction
- **Model problems give more insight**
  - Strong compressibility effect on turbulent spot growth
  - Shock amplification of upstream turbulence
  - Lack of upstream influence changes separation bubble behaviour compared to low speed flow (AI transition for strong interactions)
  - Ramps and shock impingement cases show low-frequency unsteadiness
  - Explicit compressibility terms generally small contributors to time average

References

- Adams *JFM* 420, 2000
- Ducros et al. *JCP* 152 1999
- Dupont et al *JFM* 559, 2006
- Garnier, *AIAA J* 40, 2002
- Inagaki, *J.Fluids Eng* 127, 2005
- Jocksch & Kleiser *IJHFF* 29, 2008
- Krishnan & Sandham, *JFM* 566, 2006 and *Phys Fluids* 19, 2007
- Krishnan, Sandham & Steelant *AIAA J* 47(7), 2009
- Lee, Lele & Moin, *JFM* 340, 1997
- Redford, Sandham & Roberts 2007 *DLES7*, Trieste
- Sandham, Yao and Lawal *IJHFF* 24, 2003
- Teramoto *AIAA J* 43, 2005
- Touber & Sandham *TCFD* 23, 2009
- Touber & Sandham *Shock Waves 19,* 2009
- Wu & Martin *AIAA J* 45(4), 2007
- Yao et al *Phys Fluids* 19, 2007